

The solid state of anti-inflammatory morniflumate diniflumate: a cocrystalline salt[‡]

Maria Barrio¹, René Ceolin¹, Benoit Robert^{2,§}, Hassan Allouchi,³ Jean-Marie Teulon⁴, Christophe Guéchet⁵, Josep-Lluis Tamarit¹, Ivo B. Rietveld^{2,6*}

¹ Grup de Caracterizació de Materials, Departament de Física, EEBE and Barcelona Research Center in Multiscale Science and Engineering, Universitat Politècnica de Catalunya, Eduard Maristany, 10-14, 08019 Barcelona, Catalonia.

² Normandie Université, Laboratoire SMS - EA 3233, Université de Rouen, F 76821 Mont Saint Aignan, France

³ Laboratoire SIMBA – EA 7502 et Laboratoire de Chimie Physique, Faculté de Pharmacie, Université de Tours, 31 avenue Monge – 37200 Tours, France

⁴ Jean-Marie Teulon, 78170 La Celle Saint Cloud, France

⁵ Christophe Guéchet, 30300 Fourques, France

⁶ Faculté de Pharmacie, Université de Paris, 4 avenue de l'observatoire, 75006, Paris, France

[‡] In memory of Dr Patrick Toffoli (1945-1991) and Dr Henri Szwarc (1922-2016)

* Corresponding author, e-mail: ivo.rietveld@univ-rouen.fr, current address: Neutron Science Laboratory, Institute for Solid State Physics, University of Tokyo, 5-1-5 Kashiwanoha, Kashiwa, Chiba 277-8581, Japan

§ current address: Sanofi R&D, Synthetics Platform/Early Development France, 13 quai Jules Guesde, F-94400 Vitry sur Seine, France

Abstract

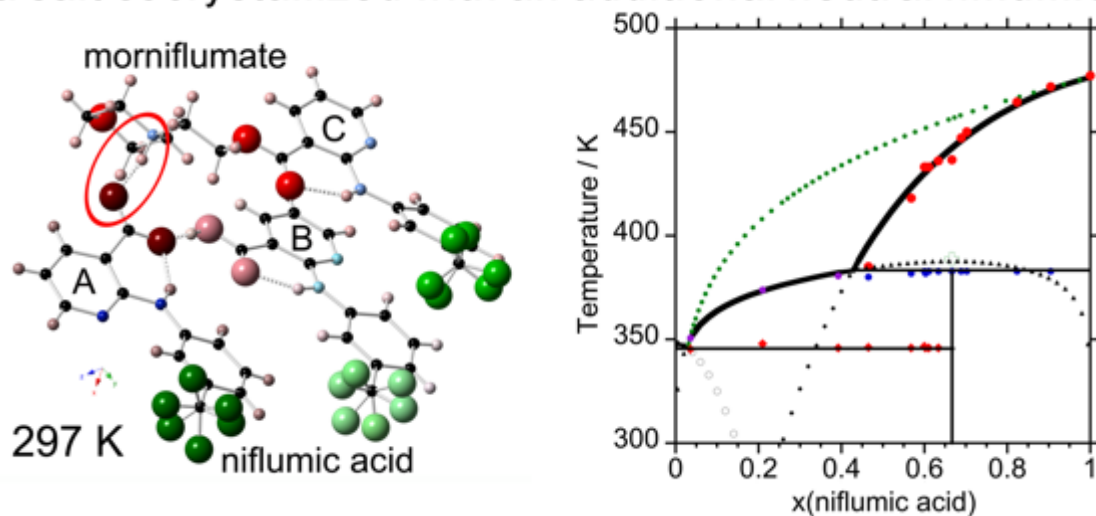
Morniflumate diniflumate, a molecular compound involving niflumic acid and its β -morpholino ethyl ester (morniflumate) in the mole ratio 2:1, is found to crystallize in a triclinic $P\bar{1}$ space group with a unit-cell volume of $2203.4(5) \text{ \AA}^3$. It is a cocrystal between a morniflumate⁺ niflumate⁻ salt and a neutral niflumic acid molecule. The co-crystalline salt forms endothermically with a positive excess volume and it melts incongruently at $382.3(8) \text{ K}$. Differential scanning calorimetry executed at heating rates above $20 \text{ K}\cdot\text{min}^{-1}$, leads to congruent melting at $387.8(9) \text{ K}$ with an enthalpy change of $\Delta_{\text{fus}}H = 80(2) \text{ J g}^{-1}$. The rare occurrence that incongruent and congruent melting can be observed for the same cocrystal may be due to the conformational versatility of the niflumic acid molecule and its slow conversion between the different conformations due to weak intramolecular hydrogen bonding.

Keywords

Anti-inflammatory, niflumic acid derivatives, cocrystal, salt, crystal structure, phase behaviour

Graphical Abstract

a salt cocrystallized with an additional neutral niflumic acid



1 Introduction

1.1 A cocrystal of niflumic acid and morniflumate

Niflumic acid with anti-inflammatory properties has a poor aqueous solubility; it falls in class II of the biopharmaceutical classification system (2011). To improve solubility, an active pharmaceutical ingredient (API) can be incorporated in a salt, because the ionic species of the API will generally have a higher solubility than the neutral compound. In addition, the incorporation of an API in a cocrystal may increase its solubility, as the mixture of water and the constituents of the cocrystal may alter the quantity of API that can be taken up in the solution.

The formation of a cocrystal with niflumic acid and morniflumate (the β -morpholino-ethyl ester of niflumic acid) was first mentioned in US and EU patents obtained in the second half of the eighties (Bru-Magniez et al., 1986, 1988). These patents describe the obtention of a crystalline compound with analgesic and anti-inflammatory properties by evaporation of ethyl ether, acetone, or methanol based solutions containing niflumic acid and morniflumate in a 2:1 molar ratio. The chemical composition of this compound is shown in **Figure 1** and its crystal structure and thermodynamic properties are described in this paper.

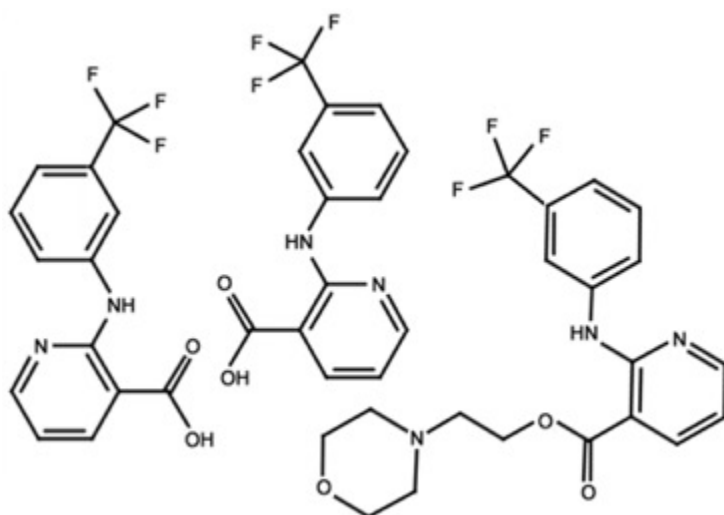


Figure 1. Morniflumate diniflumate chemical formula (left-hand side: niflumic acid, right-hand side: morniflumate molecule), $C_{45}H_{38}F_9N_7O_7$, $M = 959.82 \text{ g}\cdot\text{mol}^{-1}$

1.2 Literature data of the components niflumic acid and morniflumate

The crystal structure of niflumic acid was solved by Krishna Murthy and Vijayan in 1979 (Krishna Murthy and Vijayan, 1979). The hydrogen-atom coordinates, missing in the corresponding crystallographic information file (CIF) NIFLUM10 of the Cambridge Structural Database (CSD), can be found in the Supplementary Information **Table S1a**. The CSD contains a second CIF with the same structure, NIFLUM11, which is not linked to any publication (Surov and Perlovich, 2016). The crystal structure of morniflumate was solved by Toffoli et al. (Toffoli et al., 1988); it can be found in the CSD under the reference code GAKWIY. Furthermore, thermodynamic properties of the two chemical substances such as temperatures and heats of fusion, sublimation pressures, and density of the molten state, have been reported (Ambrus et al., 2013; Barrio et al., 2017; Perlovich et al., 2007; Pinvidic et al., 1989; Romero et al., 2004; Szunyogh et al., 2013). Available temperatures and heats of fusion of morniflumate and niflumic acid, together with new results, can be found in the Supplementary Information **Table S1b**.

2 Materials and methods

2.1 Obtention of crystalline morniflumate diniflumate

Niflumic acid and morniflumate samples from Archimica (France), purity >99.4 %, were kindly provided by Solvay (France) and used as such after verification of purity by X-ray diffraction and differential scanning calorimetry. The two compounds, mixed in a 2:1 molar ratio, were dissolved in methanol at room temperature. While the solution was slowly being evaporated, elongated platelike crystals appeared, which were dried and analysed (**Figure 2**).

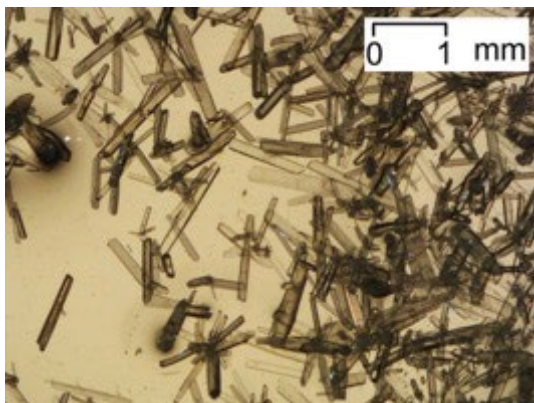


Figure 2. Optical microscopy photograph of elongated platelike crystals of morniflumate diniflumate grown from methanol at room temperature

2.2 Single-crystal X-ray diffraction

Single-crystal X-ray diffraction (SC-XRD) data were recorded on a Bruker Smart Apex diffractometer. A molybdenum $\text{I}\mu\text{S}$ microfocus X-ray source was used, running at 50 kV and 0.6 mA, emitting Mo- $\text{K}\alpha$ radiation ($\lambda = 0.710731 \text{ \AA}$). A Charge-Coupled Device (CCD chip 4K, 62 mm) area detector was positioned at 6.0 cm. The orientation matrix and unit cell were established using the APEX2 (v2014.11-0) program suite (Bruker-AXS, 2014). The 3D reflection profile and the integration of all reflections were processed with the SAINT (v8.34A) program (Bruker-AXS, 2014). The SADABS (v2014/5) program was used to correct for Lorentz and polarization effects and for absorption due to the sample (Krause et al., 2015; Sheldrick, 2014). The SHELXTL (v2014/7) program suite was used to solve the structure by the intrinsic phasing method and to refine the solution by full-matrix least-squares calculations on F^2 (Bruker-AXS, 2014). All hydrogen atoms were located using a Fourier difference map and subsequently included in the refinement with one overall isotropic thermal parameter. An Oxford Cryosystems nitrogen cryostat (Cryostream Plus) was used to carry out X-ray single crystal diffraction experiments at 100 K and at 297 K.

2.3 High-Resolution Powder X-ray Diffraction

Powder X-ray diffraction (PXRD) was carried out on a transmission mode diffractometer using Debye–Scherrer geometry equipped with cylindrical position sensitive detectors (CPS120) from INEL (France) containing 4096 channels (0.029° 2 θ -angular step) with monochromatic Cu K α_1 (λ = 1.5406 Å) radiation. Specimens were introduced in Lindemann capillaries (0.5 mm diameter) rotating perpendicularly to the X-ray beam to improve the average over the crystallite orientations. External calibration using the Na₂Ca₂Al₂F₁₄ cubic phase mixed with silver behenate was performed by means of cubic spline fittings. Measurements as a function of temperature were carried out using a liquid nitrogen 700 series Cryostream Cooler from Oxford Cryosystems.

2.4 Differential Scanning Calorimetry

Temperature (onset) and heat of transition were obtained with a Differential Scanning Calorimeter (DSC) Q100 from TA Instruments at various heating rates. The DSC was calibrated using the melting point of indium ($T_{\text{fus}} = 429.75$ K and $\Delta_{\text{fus}}H = 28.45$ J·g⁻¹). The specimens were weighed using a microbalance sensitive to 0.01 mg and sealed in aluminium pans.

2.5 Thermogravimetry

Thermogravimetric measurements were performed with a Q50 system from TA Instruments under nitrogen flux from room temperature to 550 K. Heating rates of 10 K·min⁻¹ and sample masses of ca. 5 mg were used.

3 Results and Discussion

3.1 Crystal structure

Morniflumate diniflumate has been found to crystallize in the triclinic system, centrosymmetric space group *P*-1 at room temperature. Single-crystal X-ray diffraction on these crystals has been carried out at 297 K and at 100 K. Crystal and experimental data have been compiled in **Table 1**. The CIFs can be obtained from the Cambridge Crystallographic Data Centre (CCDC), deposit numbers 2098516 and 2098518, free of charge via

www.ccdc.cam.ac.uk/data_request/cif. Atom coordinates and displacement parameters are listed in **Tables S2a and S2b** in the supplementary materials. Bond lengths and bond angles can be found in the CIFs.

Table 1. Crystal data and structure refinement for morniflumate diniflumate at 100 K and 297 K^a

Temperature $T(\sigma)$ /K	100(2)	297(2)
Crystal system	triclinic	triclinic
Space group	<i>P</i> -1	<i>P</i> -1
$a(\sigma)$ /Å	10.6111(10)	10.8037(13)
$b(\sigma)$ /Å	13.1460(13)	13.1919(16)
$c(\sigma)$ /Å	16.5222(16)	16.873(2)
$\alpha(\sigma)$ /°	75.149(1)	76.281(1)
$\beta(\sigma)$ /°	72.155(1)	71.000(1)
$\gamma(\sigma)$ /°	81.988(1)	81.859(2)
Cell Volume $V(\sigma)$ /Å ³	2115.9(4)	2203.4(5)
<i>Z</i>	2	2
<i>M</i> /g·mol ⁻¹	959.82	959.82
D_{calc} /g·cm ⁻³	1.507	1.447
V_{calc} /cm ³ ·g ⁻¹	0.66378	0.69123
μ (MoK α) /mm ⁻¹	0.129	0.124
$F(000)$	988	988
Crystal shape	rod	rod
Crystal size /mm	0.40 x 0.20 x 0.10	0.40 x 0.20 x 0.10
Radiation	MoK α ($\lambda = 0.71073$ Å)	MoK α ($\lambda = 0.71073$ Å)
θ -range /° for data collection	2.021 to 29.040	1.593 to 29.033
Completeness	0.892	0.887
Reflections collected	21774	20485
Independent reflections	10084 [$R_{\text{int}} = 0.0100$]	10411 [$R_{\text{int}} = 0.0126$]
Reflections with $I > 2\sigma(I)$	9435	8314
No. of parameters	809	849

Goodness-of-fit on F^2	1.028	1.020
Final R indexes [$\sigma \geq 2\sigma(I)$]	$R_1 = 0.0398$, $wR_2 = 0.1048$	$R_1 = 0.0456$, $wR_2 = 0.1332$
Final R indexes [all data]	$R_1 = 0.0418$, $wR_2 = 0.1067$	$R_1 = 0.0575$, $wR_2 = 0.1476$
Largest diff. peak/hole / $e \cdot \text{\AA}^{-3}$	0.787/-0.700	0.192/-0.230
CCDC	2098518	2098516

^a Estimated standard deviation (esd) in parentheses

The asymmetric unit contains one morniflumate and two niflumic acid molecules (see atom labels in **Figure S1** in the supplementary materials). The three molecules are shown in **Figure 3**. The hydrogen atom of the $-\text{COOH}$ group of niflumic acid A has moved from O2A to N3C of the morniflumate β -morpholinyl moiety. This has led to a morniflumate⁺ niflumate⁻ salt that itself has formed a cocrystal with the second, nonionized niflumic acid B. Intramolecular hydrogen bonds, which form pseudorings, and disordered $-\text{CF}_3$ groups can be observed too. They have been previously reported in niflumic acid (Krishna Murthy and Vijayan, 1979) and in morniflumate (Toffoli et al., 1988). Data on the hydrogen bonding at 297 K and at 100 K can be found in **Table S3** of the supplementary materials. On cooling to 100 K, the disorder of the morniflumate $-\text{CF}_3$ group was no longer observed (see fractional site occupancies for the F-atoms at 297 K and at 100 K in the supplementary materials **Table S4**).

The crystal structure consists of a layer with two niflumic acid molecules, the neutral niflumic acid and the niflumate cation that alternates with the negatively charged morniflumate layer. The layers stack parallel to the bc plane and normal to the \mathbf{a} axis.

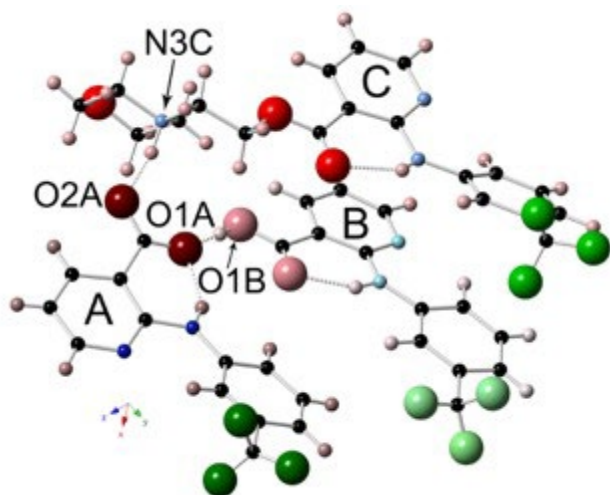


Figure 3. The molecular configuration in the cocrystal morniflumate⁺ niflumate⁻–niflumic acid at room temperature. Niflumic acid A is deprotonated and linked through a charge assisted hydrogen bond (O2A⁻⋯H—N⁺3C) with the morniflumate molecule (C). In addition, a second hydrogen bond (O1A⋯H—O1B) links it to the neutral, nonionized niflumic acid molecule B. Other hydrogen bonds, marked with dashed lines, form pseudorings virtually coplanar with the heterocycles marked by A, B, and C. Only a single orientation of each -CF₃ group is shown for clarity.

3.2 Thermal behaviour of morniflumate diniflumate

On heating the morniflumate diniflumate at various rates in a differential scanning calorimeter, unexpected thermal behaviour was recorded, as shown in **Figure 4**. At heating rates from 0.5 to 20 K·min⁻¹ from room temperature, an endothermic peak is observed at onset temperature T_1 of 382.3(8) K accompanied with an enthalpy change of 77.6(7) J·g⁻¹ when measured at rates that are larger than 0.5 K·min⁻¹. On further heating, the first peak is followed by an exothermic effect (grey area in **Figure 4**) superimposed on an endothermic effect which has a maximum at 436.6 K and is indicated by T_{\max} (see the supplementary materials **Table S5** for the values of the enthalpy changes). After cooling the molten molecular compound at a rate of -320 K·min⁻¹ to 100 K, a glass transition is observed at 301.5 K (midpoint) on reheating at a rate of 10 K·min⁻¹, which may be related to the absence of disorder observed at 100 K for the morniflumate

CF₃ moiety. The T_g can be compared with the ones found for niflumic acid at 303 K and for morniflumate at 247 K (Pinvidic et al., 1989; Romanini et al., 2019).

Thermogravimetric analysis results demonstrate no significant weight loss on heating the compound up to 450 K (see **Figure S2** in the Supplementary Materials) implying that after cooling, the individual components are still present in the system even if the cocrystal itself may have fallen apart.

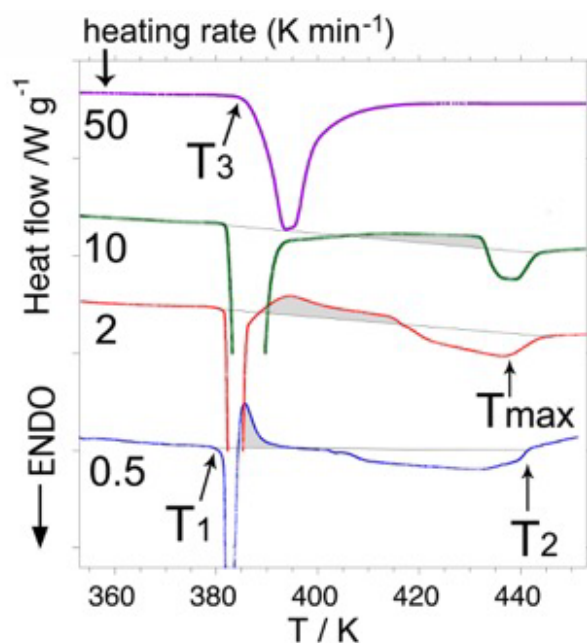


Figure 4. Differential scanning calorimetry curves recorded on heating morniflumate diniflumate cocrystals at various heating rates (see the supplementary materials **Table S5(a and b)** for quantitative information). The areas in grey correspond to the exothermic event of recrystallization of niflumic acid from the liquid of the peritectic equilibrium marked by the onset temperature T_1 . T_{max} corresponds to the maximum in the liquidus peak and T_2 corresponds to the end of the entire transition sequence.

As illustrated in **Figure 4**, the transition from the solid cocrystal to the homogeneous liquid state starts at T_1 and ends at T_2 ; according to the first principle of thermodynamics, it is accompanied with an endothermic effect of 86.1 J·g⁻¹ obtained by integration over the entire temperature range defined by the limits T_1 and T_2 (see **Table S5a** for the values). Moreover, on

heating at a rate of $50 \text{ K}\cdot\text{min}^{-1}$, a single endothermic peak is observed with an onset temperature T_3 of $387.8(9) \text{ K}$ and an enthalpy change ΔH of $80(2) \text{ J}\cdot\text{g}^{-1}$ similar in value to the more extended process below $50 \text{ K}\cdot\text{min}^{-1}$.

The combination of the DSC results in **Figure 4** (and **S2**) and powder X-ray diffraction experiments in **Figure 5** demonstrates that the phase changes evidenced by DSC correspond to the following sequence at heating rates below $20 \text{ K}\cdot\text{min}^{-1}$: (1) incongruent melting of morniflumate diniflumate with an onset at T_1 , (2) an exothermic progressive recrystallization of amorphous niflumic acid from the peritectic liquid and (3) endothermic progressive melting completed at T_2 . At $50 \text{ K}\cdot\text{min}^{-1}$, the onset of the melting of morniflumate diniflumate is observed at T_3 , which is higher than T_1 and no other effect is observed up to the final temperature of the run.

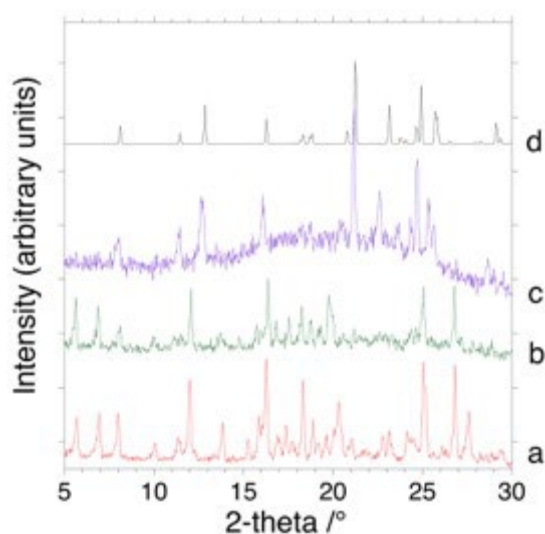


Figure 5. X-ray diffraction patterns on heating of the cocrystal morniflumate diniflumate at **(a)** 300 K, **(b)** 381.7 K, and **(c)** 389 K, the temperature at which the cocrystal has transformed into a mixture of solid niflumic acid and liquid, as indicated by the halo shape of the background. **(d)** Pattern of niflumic acid calculated at room temperature with the data published by Krishna Murthy and Vijayan (Krishna Murthy and Vijayan, 1979).

3.3 Factors influencing the morniflumate diniflumate formation

According to the Le Chatelier's principle, applying pressure favours the state of a system that possesses the smaller volume and heating favours the state of a system with the larger enthalpy. As far as the formation of the morniflumate diniflumate cocrystal is concerned, the Le Chatelier's principle can be used to evaluate the relative stability tendency of the cocrystal in relation to the temperature and the pressure if its enthalpy of formation and its excess volume are known.

3.3.1 The excess volume

At room temperature, the volume of a niflumic acid molecule is 301.80 Å³ or 301.84 Å³ (Krishna Murthy and Vijayan, 1979; Surov and Perlovich, 2016), and the volume of a molecule of morniflumate is 462.35 Å³ (Toffoli et al., 1988). According to the additivity rule, the molecular volume of the cocrystal morniflumate diniflumate should be 1066.00 Å³ (two niflumic acid molecules and one morniflumate molecule); however at 297 K, an experimental value of 1101.7 Å³ was found (see **Table 1**). The difference corresponds to a positive excess volume ΔV of +35.7 Å³ per formula unit. To confirm this result, the lattice parameters of morniflumate diniflumate at 300 K were refined using a high-resolution X-ray diffraction pattern (pattern **a** in **Figure 5**). The unit cell parameters $a = 10.834(4)$ Å, $b = 13.229(6)$ Å, $c = 16.922(8)$ Å, $\alpha = 76.175(22)$ °, $\beta = 71.014(26)$ °, $\gamma = 81.871(27)$ ° resulted in a unit-cell volume of 2221.7(1.6) Å³, i.e. 1110.85 Å³ per formula unit, leading to an even larger excess volume of $\Delta V = +44.85$ Å³.

For a more thorough investigation into the excess volume of the cocrystal's specific volume, the thermal expansion of pure morniflumate and of pure niflumic acid have been investigated using the same powder X-ray diffractometer. The temperature dependence of the morniflumate unit-cell volume had been determined previously on the same equipment (Barrio et al., 2017):

$$V_{\text{cell}}(\text{morniflumate}) / \text{Å}^3 = 890.1(1.4) + 0.0773(13) T / \text{K} + 0.000227(27) (T / \text{K})^2 \quad (1),$$

with $Z = 2$, leading to a volume of 466.8 Å³ per molecule of morniflumate at 300 K. The temperature dependence of the niflumic acid unit-cell volume has been determined for this paper by collecting

high resolution X-ray diffraction patterns between 100 K and 450 K (see the supplementary materials **Table S6**). Fitting the unit-cell volume (\AA^3) as a function of the temperature (K) leads to:

$$V_{\text{cell}}(\text{niflumic acid}) / \text{\AA}^3 = 1136.9(1.7) + 0.2678(48) T / \text{K} \quad (2);$$

hence at 300 K, the volume of a niflumic acid molecule equals 304.31\AA^3 . With these new values, a positive excess volume of $1110.85 - ((2 \times 304.31) + 466.8) = 35.4 \text{\AA}^3$ is obtained at 300 K, the same value as the initial estimate based on the single crystal data.

The same calculation can be carried out with the crystal data obtained at 100 K. Using **eqs. 1** and **2**, the molecular volume of niflumic acid at 100 K is 291\AA^3 per niflumic acid molecule and 450\AA^3 per morniflumate molecule. Following additivity, it leads to an expected volume of 1032\AA^3 per cocrystal formula-unit. Comparing this value to the experimental value of 1078.65\AA^3 in **Table 1**, a positive excess volume $\Delta V = 46.8 \text{\AA}^3$ is obtained at 100 K.

Considering that the cocrystal possesses a positive excess volume over the entire tested temperature range, it implies that an increase in pressure disfavours its formation from its individual components.

3.3.2 The heat of formation

To calculate the enthalpy of formation of the cocrystal, heat capacities of the cocrystal and its individual components are needed. The heat capacities of crystalline niflumic acid, of crystalline morniflumate and of the liquid of morniflumate can be found in a previous article (Pinvidic et al., 1989). For crystalline niflumic acid, in the temperature range from 140 K to 465 K, the heat capacity was found to be:

$$C_{p_{\text{NA(s)}}} / \text{J} \cdot \text{g}^{-1} \cdot \text{K}^{-1} = 3.19 \times 10^{-3} T / \text{K} + 0.07 \quad (3).$$

For crystalline morniflumate, in the temperature range from 110 K up to 340 K, the heat capacity was found to be:

$$C_{p_{MF(s)}} / J \cdot g^{-1} \cdot K^{-1} = 3.09 \times 10^{-3} T / K + 0.21 \quad (4),$$

while for the morniflumate liquid, in the temperature range from 356 K up to 439 K, the heat capacity is found to be:

$$C_{p_{MF(l)}} / J \cdot g^{-1} \cdot K^{-1} = 3.5 \times 10^{-3} T / K + 0.36 \quad (5).$$

Moreover, for the present paper, the specific heat of morniflumate diniflumate (NA₂MF) was determined in the solid state (140 – 382 K) and in the molten state (382 – 455 K). The mean values from three measurement series were found to be:

$$C_{p_{NA_2MF(s)}} / J \cdot g^{-1} \cdot K^{-1} = 2.97 \times 10^{-3} T / K + 0.15 \quad (6),$$

$$C_{p_{NA_2MF(l)}} / J \cdot g^{-1} \cdot K^{-1} = 3.2 \times 10^{-3} T / K + 0.34 \quad (7).$$

With these data, in combination with the melting enthalpies of its components, the enthalpy of formation of the morniflumate diniflumate cocrystal can be estimated as indicated by the thermodynamic cycle drawn in **Figure 6**.

To determine the enthalpy of formation (in J·mol⁻¹) of the morniflumate diniflumate cocrystal, $\Delta_f H$, the temperature of fusion of morniflumate MF is taken as the initial temperature ($T_i = 348.1$ K) and the melting temperature of niflumic acid NA is taken as the final temperature ($T_f = 476.2$ K). Path ΔH_1 includes the heating of solid NA₂MF from T_i to its melting temperature at 387.8 K, its heat of fusion of 80 J·g⁻¹ and the heating of the melt from 387.8 K to T_f , which gives $\Delta H_1 = 281.6$ J·g⁻¹, i.e., 270.3 kJ per mol of NA₂MF.

Path ΔH_2 includes the heating of solid niflumic acid over the entire temperature interval and its melting enthalpy of 131 J·g⁻¹, which leads to 309 J·g⁻¹, and the heat of fusion of morniflumate of 90 J·g⁻¹ and heating of the melt from T_i to T_f resulting in 321 J·g⁻¹. Hence, $\Delta H_2 = 2 \times (309 \times 282.22) + (321 \times 395.40) = 301.1$ kJ per mol of NA₂MF.

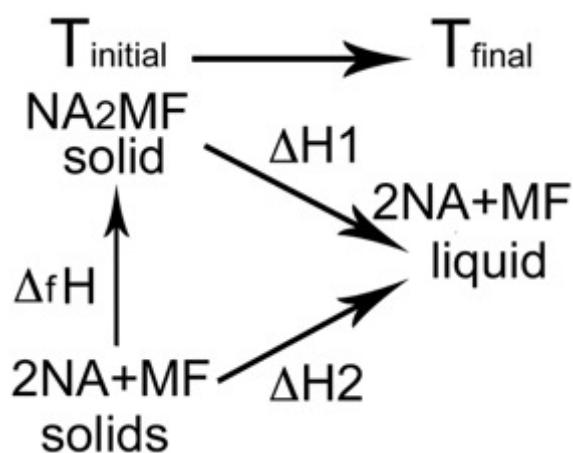


Figure 6. The thermodynamic cycle for the estimation of the enthalpy of formation $\Delta_f H$ of the morniflumate diniflumate cocrystal from its components niflumic acid ($\text{NA} \times 2$) and morniflumate (MF). Two thermodynamic paths are used from T_{initial} to T_{final} . (1) ΔH_1 : heat of fusion of NA_2MF and heating of the solid and the molten state. (2) ΔH_2 : heats of fusion of the individual components NA and MF and heating of these solids and molten states in the same temperature interval.

It follows that the heat of formation, $\Delta_f H = \Delta H_2 - \Delta H_1$, is found to be +30.8 kJ per mol of NA_2MF and it means that the formation of the cocrystal morniflumate diniflumate is endothermic, i.e., favoured by an increase in temperature. If the contributions of the specific heats are ignored and only the melting enthalpies are taken into account, a value $\Delta_f H = +32.9$ kJ per mol of NA_2MF is found, which is a difference of about 7%.

3.4 Niflumic acid-morniflumate binary system: Temperature-mol fraction ($T-x$) phase diagram

To verify whether binary compounds with other stoichiometries may exist in the niflumic acid–morniflumate system, samples were prepared by evaporating solutions of mixtures of the components in various ratios in ethyl ether at room temperature. After complete evaporation the resulting powders were examined by X-ray diffraction and differential scanning calorimetry. No other combination of the components has been found and the phase diagram in **Figure 7**,

constructed using the DSC results (see typical DSC curves in the supplementary materials **Figure S3**, the Tammann plots in **Figure S4**, and the data in **Table S7**) and the X-ray diffraction patterns of the samples, represents all phase behaviour of the morniflumate – niflumic acid system.

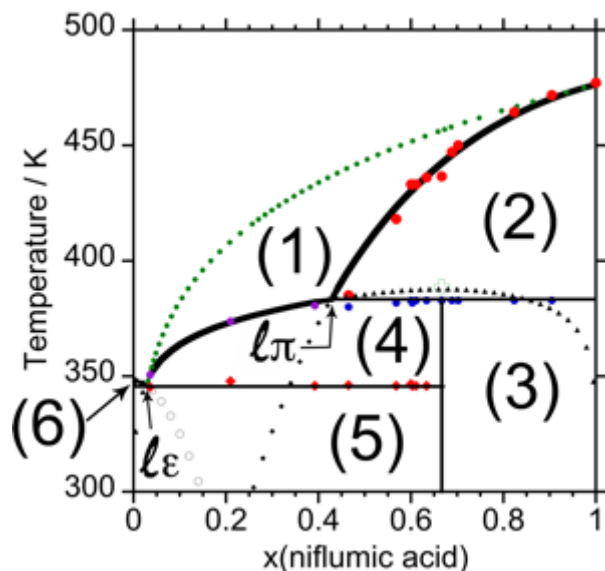


Figure 7. Morniflumate – Niflumic acid binary phase diagram. Phase regions: (1) liquid, (2) liquid + solid niflumic acid, (3) solid niflumic acid + morniflumate diniflumate, (4) liquid + morniflumate diniflumate, (5) solid morniflumate + morniflumate diniflumate, (6) liquid + solid morniflumate. $l\pi$ = peritectic liquid, $l\epsilon$ = eutectic liquid. Liquidus of niflumic acid: red solid circles with fitted line (**eq 8**), metastable extension: solid black diamonds, ideal liquidus: solid green circles. Liquidus of morniflumate: black line and metastable extension with open circles. Eutectic between morniflumate and morniflumate diniflumate: red solid diamonds with solid black line. Peritectic of morniflumate diniflumate: solid blue circles and solid black line. Liquidus of morniflumate diniflumate (**eq. 9**): stable part: violet solid circles and black solid line, metastable extensions: solid black triangles, metastable congruent melting point: open cross.

The eutectic equilibrium between morniflumate and the binary compound is found at $T\epsilon = 346.14(73)$ K, and the composition of the eutectic liquid, $x(l\epsilon) = 0.025$ (niflumic acid mol fraction),

has been estimated using the fitted liquidus lines of morniflumate and the cocrystal based on the Schroeder equation and an equation describing the thermal behaviour of compounds derived by Kuznetsov et al. (see **eq. 9** below) (Kuznetsov et al., 1975; Redlich and Kister, 1948). It demonstrates that the eutectic equilibrium is nearly degenerate with the melting temperature of pure morniflumate.

The experimental niflumic acid liquidus curve (right-hand side) does not follow ideal behaviour. The dependence of its temperature, T , on the niflumic acid mol fraction x has been fitted to the equation:

$$T_{\text{liquidus niflumic acid}} / K = (H^E(1-x)^2 - \Delta_{\text{fus}}S T_{\text{fus}}) / (-R \ln(x) + \Delta_{\text{fus}}S + S^E(1-x)^2) \quad (8)$$

based on the Redlich-Kister equation for the excess Gibbs energy in the system (Redlich and Kister, 1948). H^E is the excess enthalpy of the system in $\text{J}\cdot\text{mol}^{-1}$, $\Delta_{\text{fus}}S$, $77.3 \text{ J}\cdot\text{K}^{-1}\cdot\text{mol}^{-1}$, is the entropy of fusion of pure niflumic acid and T_{fus} , 476 K , is its melting temperature, R is the gas constant ($8.31447 \text{ J}\cdot\text{K}^{-1}\cdot\text{mol}^{-1}$) and S^E is the excess entropy of the system in $\text{J}\cdot\text{mol}^{-1}\cdot\text{K}^{-1}$. The fitting parameters H^E and S^E were found to be $-36154 \text{ J}\cdot\text{mol}^{-1}$ and $-58.6 \text{ J}\cdot\text{K}^{-1}\cdot\text{mol}^{-1}$, respectively.

The temperature of the peritectic equilibrium is found to be $382.3(8) \text{ K}$, which is the mean onset temperature T_1 of the related endothermic peaks (see **Table S5**). The composition of the peritectic liquid, $x(l\pi)$, is found to be about 0.40 (niflumic acid mole fraction) using **eq. 8** and the temperature of the peritectic equilibrium (see also the Tammann plots in Figure S4).

The liquidus of the cocrystalline salt has been fitted using an expression with variable constituents A_mB_n , with in the present case $m = 1$, and $n = 2$, leading to the following expression (Kuznetsov et al., 1975):

$$\Delta_{\text{fus}}S T_{\text{fus}} (T/T_{\text{fus}} - 1) - R T \ln(((1-x)(m+n)/m)^m (x(m+n)/m)^m) = (H^E - T S^E) (m x^2 + n (1-x)^2 - m n / (m+n)) \quad (9)$$

T_{fus} is the congruent melting point of the compound, $T_{\text{fus}} = 387.8$ K, whereas $\Delta_{\text{fus}}S$, the entropy of melting of the compound can be derived from the melting enthalpy of $80 \text{ J}\cdot\text{g}^{-1}$ ($76.8 \text{ kJ}\cdot\text{mol}^{-1}$) leading to $198 \text{ J}\cdot\text{mol}^{-1}\cdot\text{K}^{-1}$. Both values were obtained from experiment (**Table S5b**). The fitting parameters for the excess contribution H^E for the enthalpy and S^E for the entropy, were as found to be $H^E = 49.899 \text{ kJ mol}^{-1}$ and $S^E = 126.6 \text{ J}\cdot\text{mol}^{-1}\cdot\text{K}^{-1}$.

3.5 The conformations of niflumic acid and the effect on the phase behaviour

In the crystal structure of niflumic acid, two niflumic acid molecules form a hydrogen-bonded dimer, shown in the supplementary materials **Figure S5**, in which the two C=O groups are acceptors in bifurcated hydrogen bonds forming pseudo-cycles (Krishna Murthy and Vijayan, 1979). In the morniflumate diniflumate compound, one niflumic acid strongly interacts with the β -morpholino-ethyl ester (morniflumate) forming a cocrystal involving the morniflumate⁺niflumate⁻ salt moiety and an additional niflumic acid molecule. This has resulted in the removal of one of the hydrogen bonds involved in the dimer and in a proton exchange with the morniflumate in addition to a number of conformational changes illustrated in **Figure 8**.

The main change in conformation of the morniflumate molecule compared to the pure compound consists in the altered orientation of the morpholinyl group with respect to the niflumic part. Moreover, the conformation of the deprotonated niflumate cation (green, **Figure 8**) is very similar to the original conformation of niflumic acid in the pure crystal (yellow), unlike what is observed for the neutral molecule in the cocrystalline salt in magenta (**Figure 8**). The conformational change in the neutral molecule (magenta) involves the $-\text{CF}_3$ and $-\text{COOH}$ groups that are found at the same side of the molecule, while in the deprotonated molecule (green), they point in the opposite direction, similar to the conformation found in the pure acid and in the hydrated complex between niflumic acid and ethanolamine (see the supplementary materials **Figures S5** and **S6**) (Dhanaraj and Vijayan, 1983; Krishna Murthy and Vijayan, 1979).

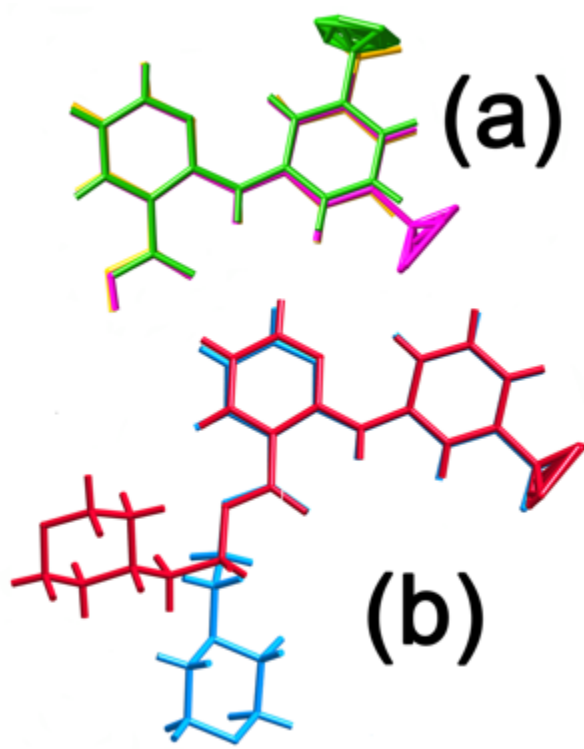
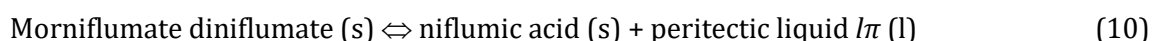


Figure 8. Conformational changes in the morniflumate diniflumate cocrystal with respect to its components. **(a)** Niflumic acid (view perpendicular to the pyridyl plane), yellow: original conformation (Krishna Murthy and Vijayan, 1979), green and magenta: conformations in the cocrystal, green (deprotonated) and magenta (neutral). **(b)** Morniflumate (view perpendicular to the phenyl ring), blue: original conformation (Toffoli et al., 1988) and red: protonated cation conformation in the cocrystal.

The experimental results demonstrate that the morniflumate diniflumate cocrystal melts incongruently at 382.3 K corresponding to a right shift in the following peritectic equilibrium:



It was observed that niflumic acid did not crystallize immediately during the shift of the equilibrium; however, it recrystallized exothermically from the peritectic liquid, depending on the heating rate (grey areas in **Figure 4**), while redissolving on further heating until a single liquid

mixture had formed at 436.8 K (i.e. the temperature of the liquidus curve at a 2:1 mole ratio of the binary phase diagram involving niflumic acid and morniflumate). Moreover, it was observed that morniflumate diniflumate melts congruently at 388 K on heating at rates above 20 K·min⁻¹, i.e. without transitory recrystallization of niflumic acid.

The observation that an incongruent peritectic melting turns into a metastable congruent melting with increasing heating rate can be explained by a kinetic energy barrier that interferes with the instantaneous reconstruction of the crystalline niflumic acid dimer from the niflumic acid molecules in the cocrystal. One of them is in need of a proton, while in the other molecule the phenyl-CF₃ group needs to rotate for 180° around the C7B-N2B bond, which is restricted by the C6B-H3B...N1B weak interaction (see **Figure S1**). It appears that niflumic acid is free to choose either the trans or cis conformation for the orientation of the CF₃ and COOH groups, while a weak interaction locks in the chosen orientation in a given crystal structure, as can be seen in the supplementary materials **Table S8** for several other structures containing niflumic acid (Bhattacharya et al., 2020; Dhanaraj and Vijayan, 1983; Fábíán et al., 2011; Hu et al., 2010; Krishna Murthy and Vijayan, 1979; Kumar et al., 2017; Mittapalli et al., 2019; Surov and Perlovich, 2016; Surov et al., 2018; Toffoli et al., 1988).

Weak hydrogen bonds involving carbon-bonded hydrogen atoms have been observed and described in other structures, and their features match those reported in **Table S8**. For instance, in 1982, Taylor and Kennard reported H...N distances in C-H...N interactions ranging from 2.522 to 2.721 Å, and they concluded that such "*contacts are attractive interactions, which can reasonably be described as hydrogen bonds*" (Taylor and Kennard, 1982). In 1984, Berkovitch-Yellin and Leiserowitz reported C...N distances in C-H...N interactions that were shorter than 3.40 Å (Berkovitch-Yellin and Leiserowitz, 1984). Similar geometries as those compiled in **Table S8** were also reported by Bosh et al. with N...H and C...N distances ranging from 2.3 to 2.6 Å and from 3.23 to 3.50 Å, respectively (Bosch et al., 2015). Moreover, the distances found in the diniflumate morniflumate cocrystal are even shorter than those found by Shivakumar et al. in aza-

heterocycles ranging from $2.574 < d(\text{H}\cdots\text{N})/\text{\AA} < 3.050$ (Shivakumar et al., 2012), and those found by Osmialowski et al. in two 2-acylaminopyrimidines with distances in the order of $2.61 < d(\text{H}\cdots\text{N})/\text{\AA} < 2.72$ and $3.387 < (\text{C}\cdots\text{N})/\text{\AA} < 3.513$ (Ośmiałowski et al., 2013).

4 Concluding remarks

The morniflumate diniflumate binary compound, formed endothermically by two niflumic acid molecules and one morniflumate molecule, has been characterized. Its crystal structure, found to be triclinic, demonstrates that it is a cocrystal between a neutral niflumic acid and a morniflumate⁻ niflumate⁺ salt. It melts incongruently at 382.3 K but it can undergo, when heated at higher heating rates, a metastable congruent melting at a higher temperature (387.8 K). As a result of its excess volume, the binary compound may fall apart under the effect of pressure. An increase of temperature has a stabilizing effect as the formation of the binary compound is endothermic; however, this stabilization is counteracted by the entropic contribution to the Gibbs energy, which starts to outweigh the enthalpy at the incongruent melting point of 382.3 K, at which temperature the binary compound ceases to be stable.

The formation of a salt combined with a neutral carboxylic acid has been observed before by Aakeröy et al. and may be a typical behaviour of carboxylate salts (Aakeröy et al., 2007). Although it may lead to unpredictability in the crystal structure as was argued in the cited article, the combined cocrystal and salt formation may nonetheless improve the solubility of the active components; thus most of these compounds should be individually investigated on their merit.

The expansivity α_v of niflumic acid, $2.36 \times 10^{-4} \text{ K}^{-1}$ from **eq. 2**, is found to be very close to the mean value of $2.21 \times 10^{-4} \text{ K}^{-1}$ for active pharmaceutical ingredients and other organic molecular solids (Céolin and Rietveld, 2015; Gavezzotti, 2013; Rietveld and Céolin, 2015). In contrast, using the cell volumes at 100 K and 297 K, a solid expansivity of $1.1 \times 10^{-4} \text{ K}^{-1}$ is found for the morniflumate diniflumate, i.e. twice as small as the usual value for solids, even if the cocrystal possesses a positive excess volume.

The solid-state studies have led to a typical phase diagram for a 1:2 molecular compound with incongruent melting or, in other words, a peritectic equilibrium. However, it is very uncommon to observe in such diagrams the metastable congruent melting too, even if some cases have been reported previously, in particular by Weinhold (Weinhold, 2009). Although kinetic factors have been indicated to explain the slow recrystallisation of pure niflumic acid above the peritectic melting transition, the observed metastability does suggest that metastable polymorphs of niflumic acid may exist that have not been observed yet.

Acknowledgements

The authors thank Marc-Antoine Perrin, a former Sanofi employee, for his assistance with data collection and scientific discussion and Anne Gonthier-Vassal, former CPMA, University of Paris Sud, for the measurements of the heat capacities. The project has been supported by the following grants: No. FIS2017-82625-P from MINECO and Project No. 2017SGR-042 from the Generalitat de Catalunya.

Declaration of Competing Interest

The authors declare the following financial interests/personal relationships which may be considered as potential competing interest: J.-M. Teulon and C. Guechot are former employees of UPSA laboratories. J.-M. Teulon is a co-author of patents EP0129449B1 and US4595686. B. Robert is at present an employee of Sanofi. The other researchers declare no competing interest.

References

2011. Martindale, The Extra Pharmacopeia, 37th ed. The Royal Pharmaceutical Society, London.
- Aakeröy, C.B., Fasulo, M.E., Desper, J., 2007. Cocrystal or Salt: Does It Really Matter? *Mol. Pharmaceut.* 4, 317-322.
- Ambrus, R., Radacsi, N., Szunyogh, T., van der Heijden, A.E.D.M., ter Horst, J.H., Szabó-Révész, P., 2013. Analysis of submicron-sized niflumic acid crystals prepared by electrospray crystallization. *J. Pharm. Biomed. Anal.* 76, 1-7.

Barrio, M., Tamarit, J.L., Ceolin, R., Robert, B., Guechot, C., Teulon, J.M., Rietveld, I.B., 2017. Experimental and topological determination of the pressure temperature phase diagram of morniflumate, a pharmaceutical ingredient with anti-inflammatory properties. *J. Chem. Thermodyn.* 112, 308-313.

Berkovitch-Yellin, Z., Leiserowitz, L., 1984. The role played by C–H···O and C–H···N interactions in determining molecular packing and conformation. *Acta Crystallogr. B* 40, 159-165.

Bhattacharya, B., Das, S., Lal, G., Soni, S.R., Ghosh, A., Reddy, C.M., Ghosh, S., 2020. Screening, crystal structures and solubility studies of a series of multidrug salt hydrates and cocrystals of fenamic acids with trimethoprim and sulfamethazine. *J. Mol. Struct.* 1199, 127028.

Bosch, E., Bowling, N.P., Darko, J., 2015. The Power of Nonconventional Phenyl C–H···N Hydrogen Bonds: Supportive Crystal-Packing Force and Dominant Supramolecular Engineering Force. *Cryst. Growth Des.* 15, 1634-1641.

Bru-Magniez, N., Teulon, J.-M., Deghenghi, R., 1986. Niflumic acid morpholinoethyl ester diniflumate, use as analgesic and anti-inflammatory agents and compositions. US4595686A.

Bru-Magniez, N., Teulon, J.-M., Deghenghi, R., 1988. Diniflumate d'ester morpholinoéthylique d'acide niflumique, préparation, utilisation en thérapeutique comme analgésique et anti-inflammatoire. EP0129449B1.

Bruker-AXS, 2014. APEX2, SAINT, SHELXTL. Bruker AXS Inc., Madison, WI, USA.

Céolin, R., Rietveld, I.B., 2015. The topological pressure-temperature phase diagram of ritonavir, an extraordinary case of crystalline dimorphism. *Ann. Pharm. Fr.* 73, 22-30.

Dhanaraj, V., Vijayan, M., 1983. A hydrated 1:1 complex between niflumic acid and ethanolamine, C₁₃H₈F₃N₂O₂·C₂H₈NO·H₂O. *Acta Crystallographica Section C* 39, 1398-1401.

Fábián, L., Hamill, N., Eccles, K.S., Moynihan, H.A., Maguire, A.R., McCausland, L., Lawrence, S.E., 2011. Cocrystals of Fenamic Acids with Nicotinamide. *Cryst. Growth Des.* 11, 3522-3528.

Gavezzotti, A., 2013. *Molecular Aggregation. Structure Analysis and Molecular Simulation of Crystals and Liquids.* Oxford University Press, Oxford, UK.

Hu, X., Gu, J., Qian, J., Wu, S., 2010. Crystal Structure of Talniflumate. *X-ray Structure Analysis Online* 26, 57-58.

Krause, L., Herbst-Irmer, R., Sheldrick, G.M., Stalke, D., 2015. Comparison of silver and molybdenum microfocus X-ray sources for single-crystal structure determination. *J. Appl. Crystallogr.* 48, 3-10.

Krishna Murthy, H.M., Vijayan, M., 1979. 2-[[3-(trifluoromethyl)phenyl]amino]-3-pyridinecarboxylic acid (niflumic acid). *Acta Crystallogr. B* 35, 262-263.

Kumar, V., Thaimattam, R., Dutta, S., Munshi, P., Ramanan, A., 2017. Structural landscape of multicomponent solids based on sulfa drugs. *CrystEngComm* 19, 2914-2924.

Kuznetsov, G.M., Leonov, M.P., Lukyanov, A.S., Kovaleva, V.A., Shapovalov, M.P., 1975. Description of Liquidus Curves of Chemical Compounds AmBn. *Dokl Akad Nauk Sssr* 223, 124-126.

Mittapalli, S., Mannava, M.K.C., Sahoo, R., Nangia, A., 2019. Cocrystals, Salts, and Supramolecular Gels of Nonsteroidal Anti-Inflammatory Drug Niflumic Acid. *Cryst. Growth Des.* 19, 219-230.

Ośmiałowski, B., Kolehmainen, E., Valkonen, A., Kowalska, M., Ikonen, S., 2013. The influence of CH bond polarization on the self-association of 2-acylaminopyrimidines by NH/CH···O/N interactions: XRD, NMR, DFT, and AIM study. *Struct. Chem.* 24, 2203-2209.

Perlovich, G.L., Surov, A.O., Bauer-Brandl, A., 2007. Thermodynamic properties of flufenamic and niflumic acids—Specific and non-specific interactions in solution and in crystal lattices, mechanism of solvation, partitioning and distribution. *J. Pharm. Biomed. Anal.* 45, 679-687.

Pinvidic, J.J., Gonthier-Vassal, A., Szwarc, H., Ceolin, R., Toffoli, P., Teulon, J.M., Guechot, C., 1989. Niflumic Acid Morniflumate Phase-Diagram .1. Study of the Components. *Thermochim. Acta* 153, 37-45.

Redlich, O., Kister, A.T., 1948. Algebraic representation of thermodynamic properties and the classification of solutions. *Ind. Eng. Chem.* 40, 345-348.

Rietveld, I.B., Céolin, R., 2015. Phenomenology of crystalline polymorphism: overall monotropic behavior of the cardiotonic agent FK664 forms A and B. *J. Therm. Anal. Calorim.* 120, 1079-1087.

Romanini, M., Rodriguez, S., Valenti, S., Barrio, M., Tamarit, J.L., Macovez, R., 2019. Nose Temperature and Anticorrelation between Recrystallization Kinetics and Molecular Relaxation Dynamics in Amorphous Morniflumate at High Pressure. *Mol. Pharmaceut.* 16, 3514-3523.

Romero, S., Bustamante, P., Escalera, B., Cirri, M., Mura, P., 2004. Characterization of the solid phases of paracetamol and fenamates at equilibrium in saturated solutions. *J. Therm. Anal. Calorim.* 77, 541-554.

Sheldrick, G.M., 2014. APEX2 Software Suite for Crystallographic Programs. Bruker AXS Inc., Madison, WI, USA.

Shivakumar, K., Vidyasagar, A., Naidu, A., Gonnade, R.G., Sureshan, K.M., 2012. Strength from weakness: The role of CH...N hydrogen bond in the formation of wave-like topology in crystals of aza-heterocycles. *CrystEngComm* 14, 519-524.

Surov, A.O., Perlovich, G.L., 2016. 2-((3-(trifluoromethyl)phenyl)amino)nicotinic acid. Private Communication to the CSD.

Surov, A.O., Voronin, A.P., Vener, M.V., Churakov, A.V., Perlovich, G.L., 2018. Specific features of supramolecular organisation and hydrogen bonding in proline cocrystals: a case study of fenamates and diclofenac. *CrystEngComm* 20, 6970-6981.

Szunyogh, T., Ambrus, R., Szabó-Révész, P., 2013. Nanonization of Niflumic Acid by Co-Grinding. *Advances in Nanoparticles* 02, 329-335.

Taylor, R., Kennard, O., 1982. Crystallographic evidence for the existence of CH.cntdot.cntdot.cntdot.O, CH.cntdot.cntdot.cntdot.N and CH.cntdot.cntdot.cntdot.Cl hydrogen bonds. *J. Am. Chem. Soc.* 104, 5063-5070.

Toffoli, P., Coquillay, M., Rodier, N., Ceolin, R., Teulon, J.M., Guehot, C., 1988. Morpholinoethyl Niflumate (DCI: Morniflunate). *Acta Crystallogr. C* 44, 547-550.

Weinhold, F., 2009. *Classical and Geometrical Theory of Chemical and Phase Thermodynamics*. John Wiley & Sons.